Available online at www.sciencedirect.com
ScienceDirect
Journal of the European Ceramic Society 30 (2010) 165–169
www.elsevier.com/locate/jeurceramsoc

Melt synthesis of Eu-doped oxide phosphors using arc-imaging furnace

Tadashi Ishigaki [a,b,*], Masahiro Yoshimura [a], Nobuhiro Matsushita [a], Kazuyoshi Uematsu [c], Kenji Toda [b,d], Mineo Sato [b,c]

[a] *Materials and Structures Laboratory, Tokyo Institute of Technology, 4259 Nagatsuta, Midori, Yokohama 226-8503, Japan*
[b] *Center for Transdisciplinary Research, Niigata University, 8050 Ikarashi 2-nocho, Nishi-ku Niigata 950-2181, Japan*
[c] *Department of Chemistry and Chemical Engineering, Niigata University, 8050 Igarashi 2-nocho, Nishi-ku Niigata 950-2181, Japan*
[d] *Graduate School of Science and Technology, Niigata University, 8050 Igarashi 2-nocho, Nishi-ku Niigata 950-2181, Japan*

Available online 1 July 2009

Abstract

To synthesize various complex oxide materials and their solid solutions, we applied a novel "melt-synthesis technique" rather than conventional solid-state reaction techniques. Rapid synthesis methods to develop those double oxides have been strongly anticipated. During melt synthesis, the mixture of oxides or their precursors is melted rapidly (1–60 s) in an arc-imaging furnace using strong light radiation. A spherical molten sample with multiple homogeneously mixed cations was solidified directly on a copper hearth with rapid cooling of ca. 10^2 °C/s.

We studied the synthesis of A_2BO_4 type double oxides $(AA')_2BO_4$ ($A = Sr^{2+}$, Ca^{2+}, $A' = La^{3+}$, Gd^{3+}, Y^{3+}, Eu^{3+}, $B = Al$) using this method. Homogeneous samples with Eu^{3+} dopants were synthesized using liquid phase mixing in a few seconds, which is much faster than diffusions of ions in solid phase. Red fluorescence under the irradiation of ultraviolet light (254 and 365 nm) was observed. The excitation band shifted.

Keywords: Melt synthesis; Phosphors; Perovskite K_2NiF_4-type; Y_2O_3:Eu

1. Introduction

Complex oxide compounds such as perovskite-type ABO_3, spinel-type AB_2O_4 and sheelite-type ABO_4 materials have been investigated in such widely diverse fields as ferroelectrics, magnetics, optics, phosphors, electronics, ionics, superconductors, sensors, and catalysts because they have various but unique properties attributable to their compositions and structures, which are characterized by their various combinations of constituent A and B ions.

Recently, we investigated a series of complex perovskites – $(AA')(BB')O_3$ perovskites – using a melt-synthesis method, demonstrating that it is an easy route to make such perovskite solid solutions.[1] We extended these studies to a series of ternary mixed oxides of the composition of $AA'BO_4$, structurally related to K_2NiF_4. Such complex oxides are not easy to synthesize using conventional solid-state reaction techniques because the reaction rates among oxides are so slow by solid-state diffusions to form homogeneous compounds or solid solutions. In contrast, melt reactions are extremely rapid and homogeneous because of liquid mixing and rapid diffusion in the liquid phase, in contrast to conventional solid-state reactions. These melt-synthesis techniques are therefore suitable for synthesizing multi-component compounds and solid solutions where homogeneous cation mixing is required.

Moreover, the melt synthesis has another interesting feature because it is a high-temperature approach for synthesis, which is rather opposite from solid-state syntheses. The latter is a low-temperature approach to the synthetic temperature: the melt-synthesis might produce metastable phases at higher temperatures, which might not be formed by the solid-state reactions even for a long heating. However, the melt synthesis has not been studied widely yet, probably because it is not easy to produce such high temperatures or obtain a non-reactive container to molten oxides at such a high temperature as 1500–2000 °C. Using an arc-imaging furnace, however, we synthesized a series of perovskite-type phases in systems of $GdScO_3$–$BaTiO_3$, –$SrTiO_3$, –$CaTiO_3$, $LaAlO_3$–$BaTiO_3$, –$SrTiO_3$, and –$CaTiO_3$, which are solid solutions in the systems of $A^{2+}B^{4+}O_3$–$A^{3+}B^{3+}O_3$.[2] Melting using an arc-imaging furnace requires no container at various atmospheres up to high temperatures even greater than 2000 °C.[3,4]

* Corresponding author at: Center for Transdisciplinary Research, Niigata University, 8050 Ikarashi 2-nocho, Nishi-ku Niigata 950-2181, Japan.
Tel.: +81 25 262 7760; fax: +81 25 262 7760.
E-mail address: tishigaki@eng.niigata-u.ac.jp (T. Ishigaki).

0955-2219/$ – see front matter © 2009 Elsevier Ltd. All rights reserved.
doi:10.1016/j.jeurceramsoc.2009.05.040

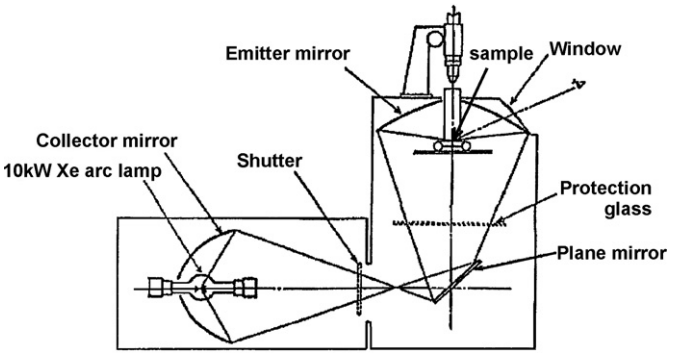

Fig. 1. Optical system of the arc-imaging furnace. The light source is a xenon arc lamp. The light is reflected from a collection mirror, a plane mirror, and an emission mirror to heat a sample on a sample stage.

Combining those advantages of the melt synthesis and the arc-imaging furnace, we have undertaken in the present study to prepare Y_2O_3:Eu^{3+} and K_2NiF_4-type solid solutions for phosphors rapidly, where homogeneous Eu^{3+} doping is strongly required.[3,4]

2. Experimental

2.1. Arc-imaging furnace

This furnace is designed to heat small samples to very high temperatures such as those higher than 2000 °C to melt in clean conditions. As presented in Fig. 1, the light emitted from a 10 kW xenon lamp is collected using an ellipsoidal mirror (collector), reflected using a plane mirror, and then emitted by another ellipsoidal mirror (emitter) to the sample. A 3–8 mm moulded sample of mixed powders was put on a water-cooled Cu hearth. In various atmospheres, the sample can be heated rapidly up to the melting temperature – in just a few seconds – and also cooled by breaking the light radiation using a shutter or quickly removing the sample stage from the emitter mirror's focus. The brightness temperature can be monitored using a pyrometer. To calibrate this pyrometry system, the solidification temperatures of refractory oxides were measured as Al_2O_3 (2054 ± 4 °C), Y_2O_3 (2433 ± 3 °C), HfO_2 (2803 ± 3 °C), and CaO (2899 ± 3 °C).[3,4] Details of the furnace and the pyrometry were reported in earlier papers.[3,4] When a sample is melted, it becomes a small (1–5 mm) molten globule because of its surface tension; thereby it gives almost point-contact to the Cu hearth, which minimizes the heat loss by the hearth. When the bottom of the sample is unmolten, the sample can be remelted after it is turned over.

2.2. Sample preparation

Starting materials were high purity carbonates and oxides ($SrCO_3$ (99.9%, Kojundo Chemical Lab. Co.), $BaCO_3$ (99.95%, Kojundo), $CaCO_3$ (99.5%, Kanto Kagaku Co., Ltd.), Al_2O_3 (99.99%, AKP-30; Sumitomo Chemical Co. Ltd.), Eu_2O_3 (99.99%, Shin-Etsu Chemical Co.), Gd_2O_3 (99.99%, Shin-Etsu), La_2O_3 (99.99%, Shin-Etsu), and Y_2O_3 (99.99%, Shin-Etsu)) powders. They were mixed using dry and wet mixing in a high-purity alumina mortar. The mixed powders or their moulded samples were placed on the copper hearth and melted at normal pressures using the arc-imaging furnace. It generally took 5–15 s from a molten state at around 2000 °C to a solid state with dark colour at around 600 °C. The cooling rate was estimated as more than 100 °C/s.

All samples were characterized using X-ray diffraction. Powder X-ray diffraction patterns were obtained from arc-melted samples after grinding using an alumina mortar, with Cu Kα radiation in a curved graphite-beam monochrometer (MXP3VA; Mac Science Ltd., Tokyo, Japan).

A spectrofluorometer (F-4500; Hitachi Ltd.) equipped with a 150 W Xe-arc lamp was used for the photoluminescence (PL) measurement at a room temperature for the sample loaded on powder.

3. Results and discussion

3.1. Y_2O_3:Eu^{3+} melted samples

A Y_2O_3:Eu^{3+} solid solution with $0.005 < x < 0.15$ in $(Y_{1-x}Eu_x)_2O_3$ was synthesized rapidly (5–60 s) using the melt method in a single step from the mixed powders. The 5 mm diameter sample is globular.

It is a notable merit of melt synthesis that solid-state synthesis generally requires repeated multiple steps such as powder moulding to a pellet, heating to high temperatures, and grinding to powder. For example, a study of Y_2O_3:Eu^{3+} by Ozawa[5] reported the synthesis temperature as 1300 °C and 3 h calcination. Forest and Ban synthesized Y_2O_3:Eu^{3+} from oxalates at 1400 °C for 2 h.[6] Another advantage of melt synthesis is that it avoids contamination from grinding media and containers during grinding.

Many reports describe synthesis of homogeneous Y_2O_3:Eu^{3+} phosphors using solution processes.[7–10] These solution processes have multiple steps with sophisticated reactions. Ozawa reported[7] preparation of the material by dissolving the rare earth oxide in hot nitric acid, with subsequent precipitation using oxalic acid and finally firing at 1200 °C for 2 h.

Fig. 2 portrays X-ray powder diffraction patterns of Y_2O_3:Eu^{3+} samples, which indicated that all the samples were of cubic single phase. The peaks shifted to lower angles concomitantly with increasing contents of Eu^{3+}.

Because Eu^{3+}(0.947 nm) has a slightly larger ionic radius than Y^{3+}(0.900 nm), the doping of Eu^{3+} increases the lattice parameters as well as the cell volumes of the solid solutions, as shown in Fig. 3. The present results closely resemble the reported ones $a = 1.06041$ nm for pure Y_2O_3,[11] but are slightly larger than that (1.060 nm) for $(Y_{0.95}Eu_{0.05})_2O_3$.[12]

The latter is somewhat strange because it is rather smaller than pure Y_2O_3, even with larger Eu^{3+} ions. Here we demonstrate that the melt synthesis is rapid and homogeneous reactions because ions are mixed more homogeneously in the melt than in the solid.

Even the melt shows a random distribution of anions and cations. However, the local coordination of the anions and the cations is expected to be almost identical to that in the crystalline

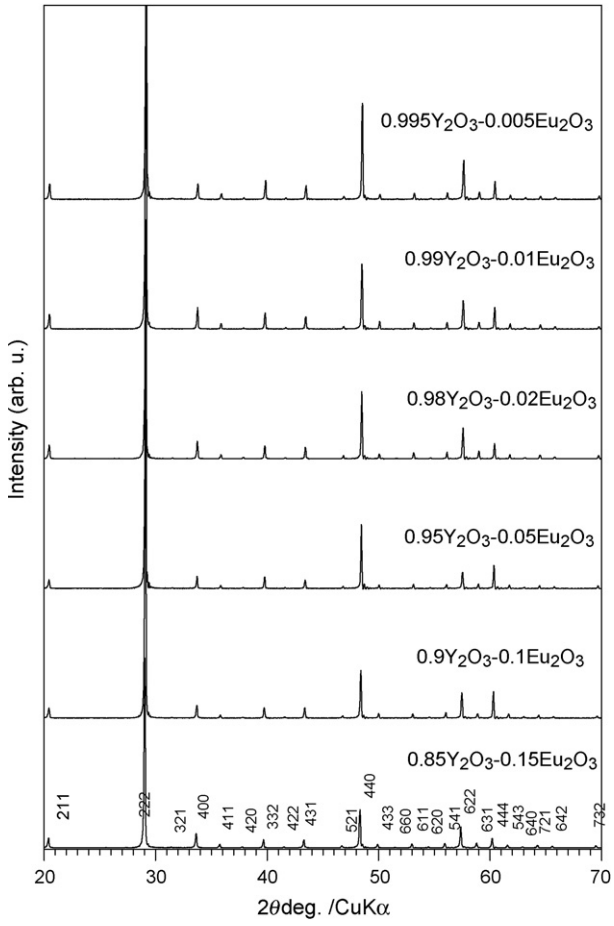

Fig. 2. XRD pattern of the melt-synthesized Eu^{3+}-doped Y_2O_3 samples. Peaks were identified using JCPDS #25-1014.

solid: the coordination number of the Y site is 6, and the O site's is 4, as in the C-type structure crystal. If all the anions and cations were able to mix randomly, then a huge volume change would be observed when the melt was crystallized, but such changes have never been reported.

Emission spectra of Y_2O_3:Eu^{3+} samples are presented in Fig. 4 as a function of the amount of doped Eu^{3+} components.

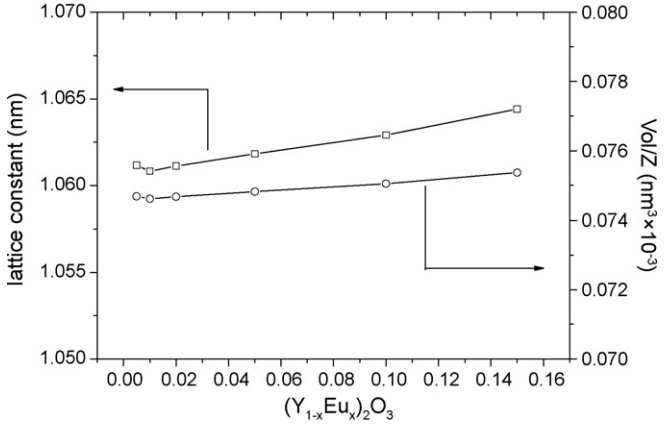

Fig. 3. Lattice parameter cell volume of the melt-synthesized Eu^{3+}-doped Y_2O_3 samples.

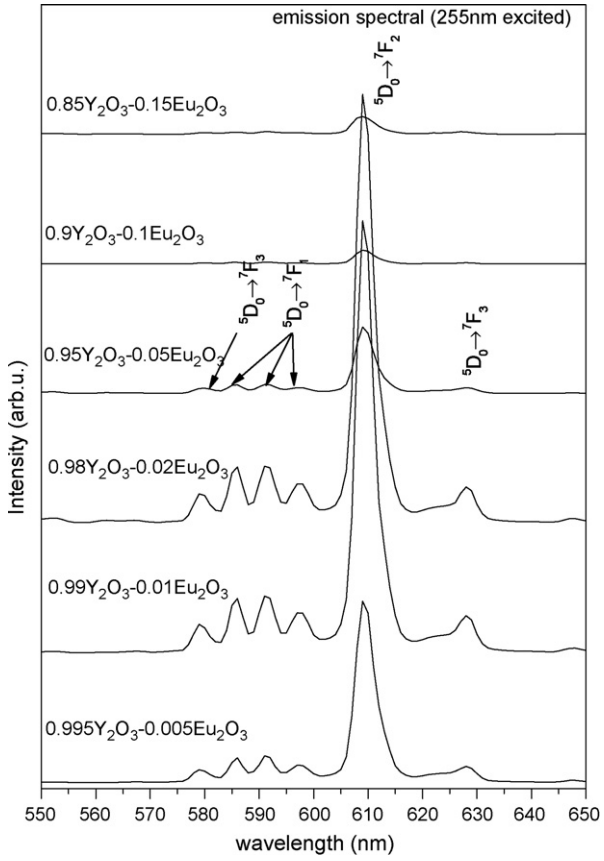

Fig. 4. Emission spectra of the melt-synthesized Eu^{3+}-doped Y_2O_3 samples (excited 225 nm).

When the Y_2O_3:Eu^{3+} phosphor samples were excited by the radiation of 255 nm narrow-band red emission extending from 590 to 700 nm with a sharp peak at 611 nm, corresponding to the $^5D_0 \rightarrow {}^7F_2$ transition of the Eu^{3+} ion was observed. The Y_2O_3:Eu^{3+} has been used as a red fluorescent material since the 1960s.[13–15] According to these reports, every peak is identifiable as depicted in Fig. 4. Moreover, the emission wavelength is independent of the Eu^{3+} concentration. The emission at wavelength at 611 nm shows an increase concomitantly with the increases in the Eu^{3+} concentration up to 0.01, but a further increase of concentration decreased the emissions because of concentration quenching, as described in an earlier report.[16]

3.2. *Melted $AA'AlO_4$:Eu samples*

Homogeneous A_2BO_4 type compounds were also produced using rapid synthesis via melting using the arc-imaging furnace.

Fig. 5 presents X-ray powder diffraction patterns of $SrLaAlO_4$ and $Sr(La_{0.85}Eu_{0.15})AlO_4$ samples, each of which was found to have a well-crystallized K_2NiF_4-type single phase in comparison with standard Ref. 17. Other cation combinations of A (Ca, Sr, Ba) and A′(Y, Gd, La) also brought about similar structured phases.

Table 1 presents the lattice parameters and ionic radius ratio $r_{A'}/r_A$ of $AA'AlO_4$ compounds with A (=Ca, Sr, Ba) and A′ (=Y, Gd, La). The lattice parameter of the $A(La_{0.85}Eu_{0.15})AlO_4$ is

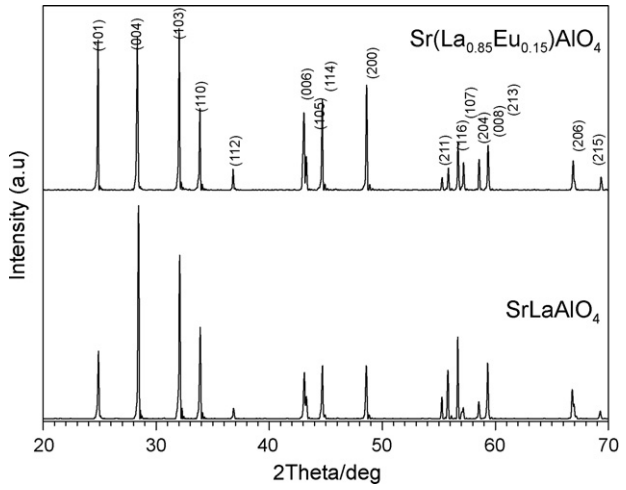

Fig. 5. XRD pattern of the melt synthesized $SrLaAlO_4$ and Eu^{3+}-doped $SrLaAlO_4$ samples. Peaks were identified using JCPDS #24-1125.

reported herein for the first time: their crystal systems depend on the ionic radius ratio, i.e., the value of $r_{A'}/r_A$ is greater than 0.85; the tetragonal-K_2NiF_4 phases are formed for $r_{A'}/r_A \geq 0.85$, although orthorhombic-K_2NiF_4 phases exist around $r_{A'}/r_A = 0.83$ but not the single phase for $r_{A'}/r_A \leq 0.82$.

Fig. 6 shows the $AA'AlO_4$ cell volume as a function of the A-ion radius. The ionic radii of Y^{3+}, Gd^{3+}, Eu^{3+}, and La^{3+} are, respectively, 0.1075, 0.1107, 0.1120, and 0.1216, with the nine coordination number for the A or A′ site. Because smaller Eu substitutes for La in solid solutions, $A(La_{0.85}Eu_{0.15})AlO_4$ has smaller volume than $ALaAlO_4$.

The emission spectra of $A(A'_{0.85}Eu_{0.15})AlO_4$ samples are presented in Fig. 7. The room temperature emission spectra for every compound were compared. As with the Y_2O_3:Eu^{3+} compound case, the rare-earth-doped compounds have received much attention because of their high luminescence efficiencies.

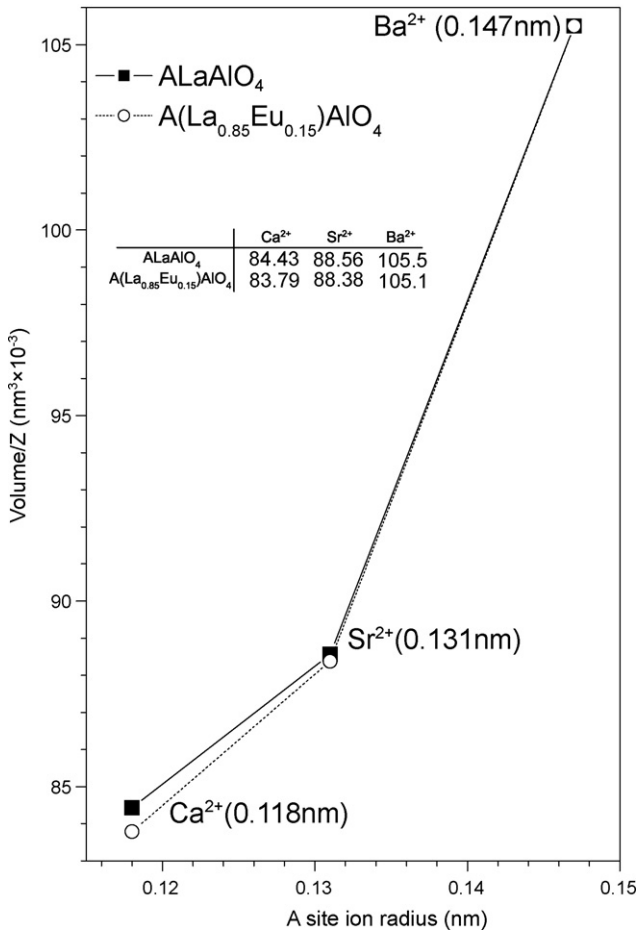

Fig. 6. $ALaAlO_4$, $A(La_{0.85}Eu_{0.15})AlO_4$, (A = Ca, Sr, Ba) cell volume. The $A(La_{0.85}Eu_{0.15})AlO_4$ volume is smaller than that of $ALaAlO_4$. Because Eu ion < La ion, europium solid solutions must have been produced.

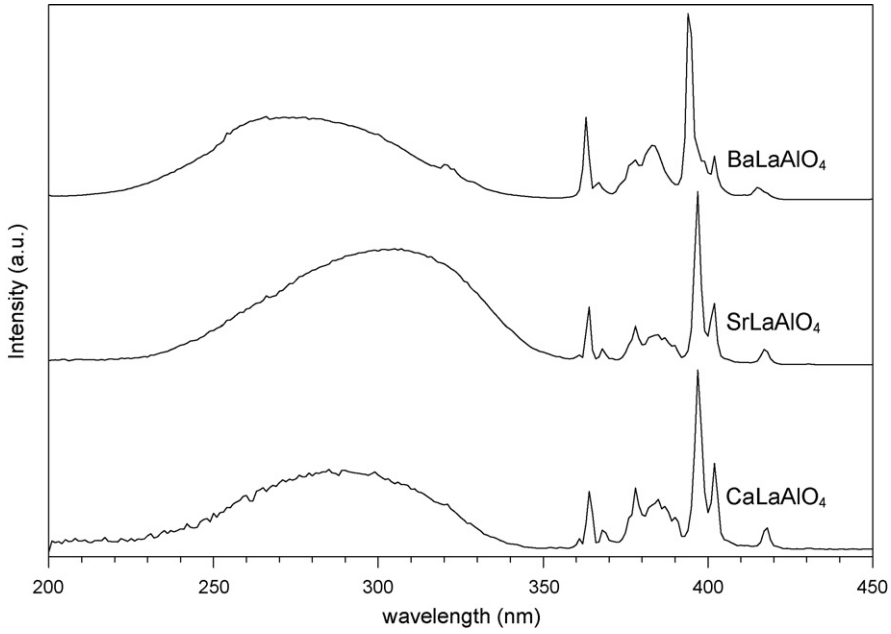

Fig. 7. Excitation spectra of emission 610 nm for $ALaAlO_4$, $A(La_{0.85}Eu_{0.15})AlO_4$, and (A = Ca, Sr, Ba) compounds.

Table 1
Formation diagram $AA'AlO_4$ phase. The horizontal column shows alkaline earth ions in the A site. The vertical column shows rare earth ions in the A′ site.

A′ site	A site		
	Ca^{2+} (0.118 nm)	Sr^{2+} (0.131 nm)	Ba^{2+} (0.147 nm)
Y^{3+} (0.108 nm)	0.92	0.82	0.73
Gd^{3+} (0.111 nm)	0.94	0.85	0.76
La^{3+} (0.122 nm)	1.03	0.93	0.83

Because of concentration quenching, an excessive doping of emission ions would generally decrease the emission intensity markedly. The K_2NiF_4-type layered perovskite structure comprises a two-dimensional arrangement of the rare earth ions. These low-dimensional arrangements of the rare earth ions enable their long separations.[18] Moreover, according to Honma et al.,[19] the low-dimensional arrangement of the emission ions might alleviate contact with killers, such as impurities or vacancies, and a heavier framework is expected to reduce the non-radiative relaxation of the excitation energy through phonons.

The excitation spectra of the charge transfer band (CTB) (250–340 nm) were broadened, showing a shift from 270 to 310 nm (red shift). In turn, the emission spectra showed a slight blue shift. This red shift in the charge transfer band can be considered by the increase in the lattice volume. Actually, CTB corresponds to an electron transfer from an oxygen 2p orbital to an empty orbital of europium. The position of the band regularly shifted with the change of the local structure of the rare-earth ions. The position of the CTB tends to become lower with increasing coordination number[10] and is strongly dependent on the Eu–O distance.[13] With increasing bond length, the band shifts to lower energies. Consequently, the reason for the red shift in CTB is not only the lattice volume but also the Eu–O distance because of the lattice symmetry, i.e., the tetragonal compounds $SrLaAlO_4:Eu^{3+}$ and $CaLaAlO_4:Eu^{3+}$ respectively have a distance of 2.48 and 2.38 Å.[20,21] For $BaLaAlO_4:Eu^{3+}$ a red shift is suspected because of symmetric difference, direct excitation peaks of orthorhombic $BaLaAlO_4:Eu^{3+}$ had higher energy than tetragonal $SrLaAlO_4:Eu^{3+}$ or $CaLaAlO_4:Eu^{3+}$.

4. Conclusions

- Homogeneous $Y_2O_3:Eu^{3+}$ and $A_2BO_4:Eu^{3+}$ compounds of K_2NiF_4-type were produced through rapid synthesis via the melt process using an arc-imaging furnace.
- Emission properties of $Y_2O_3:Eu^{3+}$ are almost identical to those described in previous reports.
- In $(AA')AlO_4$ compounds, the tetragonal phase in the case of $r_{A'}/r_A > 0.85$ fed the orthorhombic phase for $r_{A'}/r_A \approx 0.83$, but no single compounds for $r_{A'}/r_A < 0.82$.
- The CTBs of $Ca(La_{0.85}Eu_{0.15})AlO_4$ and $Sr(La_{0.85}Eu_{0.15})AlO_4$ were, respectively, 285 and 310 nm.
- In fact, A_2BO_4 type compounds can be used as phosphor materials.

Acknowledgements

The authors thank Eiichiro Nishimura, and Kazumasa Seki for their assistance on this research. Photoluminescence measurement equipment-related aspects of this work were supported by Prof. Yamase and Dr. Itoh at the Chemical Resources Laboratory, Tokyo Institute of Technology, Japan.

References

1. Ishigaki, T., Seki, K., Nishimura, E., Watanabe, T. and Yoshimura, M., Melt synthesis and characterization of complexed oxide perovskites containing rare earths. *J. Alloys Compd.*, 2006, **408–412**, 1177–1181.
2. Ishigaki, T., Nishimura, E., Seki, K., Watanabe, T. and Yoshimura, M., Melt synthesis and characterization of complexed perovskite-oxides in the system of $A^{2+}(B^{+}_{2/5}B^{6+}_{3/5})O_3$–$A^{3+}(B^{+}_{3/5}B_{2/5}{}^{6+})O_3$. *J. Electroceram.*, 2006, **17**, 885–889.
3. Yamada, T., Yoshimura, M. and Somiya, S., Redetermination of the solidification points of Al_2O_3, Y_2O_3, and HfO_2 by digital pyrometry with an arc-imaging furnace. *High Temp. High Press.*, 1986, **18**, 377–388.
4. Yamada, T., Yoshimura, M. and Sōmiya, S., Reinvestigation of the solidification point of CaO by digital pyrometry. *J. Am. Ceram. Soc.*, 1986, **69**, C243–C245.
5. Ozawa, L., Emission and excitation spectra of Eu_2O_3 compared with Y_2O_3:Eu phosphor. *Jpn. J. Appl. Phys.*, 1966, **5**, 740–741.
6. Forest, H. and Ban, G., Random substitution of Eu^{3+} for Y^{3+} in $Y_2O_3:Eu^{3+}$. *J. Electrochem. Soc.*, 1971, **118**, 1999–2001.
7. Ozawa, L., Forest, H., Jaffe, P. M. and Ban, G., Random substitution of Eu^{3+} for Y^{3+} in $Y_2O_3:Eu^{3+}$. *J. Electrochem. Soc.*, 1971, **118**, 482–486.
8. McKittrick, J., Lopez, O. A. and Sluzky, E., Synthesis of red-emitting. Small particle size luminescent oxides using an optimized combustion process. *J. Am. Ceram. Soc.*, 1996, **79**, 3257–3265.
9. Guo, H., Zhang, W., Lou, L., Brioude, A. and Mugnier, J., Structure and optical properties of rare earth doped Y_2O_3 waveguide films derived by sol–gel process. *Thin Solid Films*, 2004, **458**, 274–280.
10. Zhang, K., Pradhan, A. K., Loutts, G. B., Utpal, N. R., Cui, Y. and Burger, A., Enhanced luminescence and size effects of $Y_2O_3:Eu^{3+}$ nanoparticles and ceramics revealed by X rays and Raman scattering. *J. Opt. Soc. Am. B*, 2004, **12**, 1804–1808.
11. International Centre for Diffraction Data JCPDS #41-1105.
12. International Centre for Diffraction Data JCPDS #25-1011.
13. Chang, N. C., Fluorescence and stimulated emission from trivalent europium in yttrium oxide. *J. Appl. Phys.*, 1963, **34**, 3500–3504.
14. Chang, N. C. and Gruber, J. B., Spectra and energy levels of Eu^{3+} in Y_2O_3. *J. Chem. Phys.*, 1964, **41**, 3227–3234.
15. Wickersheim, K. A. and Lefever, R. A., Luminescent behavior of the rare earths in yttrium oxide and related hosts. *J. Electrochem. Soc.*, 1964, **111**, 47–51.
16. Kwak, M.-G., Park, J.-H. and Shon, S. H., Synthesis and properties of luminescent Y_2O_3:Eu (15–25 wt%) nanocrystals. *Solid State Commun.*, 2004, **130**, 199–201.
17. International Centre for Diffraction Data JCPDS #24-1125.
18. Kudo, A. and Sakata, T., Luminescent properties of nondoped and rare earth metal ion-doped $K_2La_2Ti_3O_{10}$ with layered perovskite structures: importance of the hole trap process. *J. Phys. Chem.*, 1995, **99**, 15963–15967.
19. Honma, T., Toda, K., Ye, Z.-G. and Sato, M., Concentration quenching of the Eu^{3+}-activated luminescence in some layered perovskites with two-dimensional arrangement. *J. Phys. Chem. Solids*, 1998, **59**, 1187–1193.
20. Magrez, A., Morniroli, J. P., Caldes, M. T., Marie, A. M., Joubert, O. and Brohan, L., Using CBED and crystallographic image processing to evidence a structural distortion in a new family of ionic conductor $Sr_{1-x}La_{1+x}Al_{1-x}Mg_xO_4$ $(0 \le x \le 0.7)$. *J. Solid State Chem.*, 2003, **172**, 243–251.
21. Levin, A. A., Butikova, I. K. and Smolin, Yu. I., Crystal structure of $CaLaAlO_4$. *Zh. Neorg. Khim.*, 1998, **43**, 718–720.